11878–11890 *Nucleic Acids Research, 2017, Vol. 45, No. 20* *Published online 20 October 2017*
doi: 10.1093/nar/gkx939

RecQ helicase triggers a binding mode change in the SSB–DNA complex to efficiently initiate DNA unwinding

Maria Mills[1,†], Gábor M. Harami[2,†], Yeonee Seol[1], Máté Gyimesi[2], Máté Martina[2], Zoltán J. Kovács[2], Mihály Kovács[2,*] and Keir C. Neuman[1,*]

[1]Laboratory of Single Molecule Biophysics, National Heart, Lung and Blood Institute, National Institutes of Health, Bethesda, MD 20892, USA and [2]Department of Biochemistry, ELTE-MTA "Momentum" Motor Enzymology Research Group, Eötvös Loránd University, Pázmány P. s. 1/c, H-1117 Budapest, Hungary

Received May 23, 2017; Revised September 29, 2017; Editorial Decision October 03, 2017; Accepted October 09, 2017

ABSTRACT

The single-stranded DNA binding protein (SSB) of *Escherichia coli* plays essential roles in maintaining genome integrity by sequestering ssDNA and mediating DNA processing pathways through interactions with DNA-processing enzymes. Despite its DNA-sequestering properties, SSB stimulates the DNA processing activities of some of its binding partners. One example is the genome maintenance protein RecQ helicase. Here, we determine the mechanistic details of the RecQ–SSB interaction using single-molecule magnetic tweezers and rapid kinetic experiments. Our results reveal that the SSB–RecQ interaction changes the binding mode of SSB, thereby allowing RecQ to gain access to ssDNA and facilitating DNA unwinding. Conversely, the interaction of RecQ with the SSB C-terminal tail increases the on-rate of RecQ–DNA binding and has a modest stimulatory effect on the unwinding rate of RecQ. We propose that this bidirectional communication promotes efficient DNA processing and explains how SSB stimulates rather than inhibits RecQ activity.

INTRODUCTION

Single-stranded DNA binding proteins (SSBs) play essential roles in genome maintenance. SSB binds single-stranded DNA (ssDNA) in a sequence independent manner and sequesters ssDNA from other proteins, preventing non-specific protein binding, secondary DNA structure formation, and ssDNA degradation (1–5). In addition to this important but passive role, SSB recruits enzymes associated with DNA metabolism to their target sites and stimulates their catalytic activities (6–11). Examples of proteins associated with bacterial SSBs include RecA (12), PriA helicase (6,13,14), Exonuclease I (9), RecO (11,15), RecG (16) and RecQ helicase (7,17).

The prototypical bacterial single-stranded DNA binding protein, *Escherichia coli* SSB, is a homotetramer in which each monomer consists of a DNA-binding OB fold and an unstructured C-terminal tail (18–20). *In vitro*, SSB is known to interact with ssDNA in different binding modes (21–24). In the two best-characterized of these modes, either 65 or 35 nucleotides (nt) of ssDNA are wrapped around the SSB molecule. The crystal structure of SSB bound to ssDNA suggests a model in which the DNA is wrapped around all four subunits in the 65-nt binding mode and, on average, two subunits in the 35-nt binding mode (19) (Figure 1). Interconversion among different binding modes has been detected in both single-molecule FRET and single-molecule manipulation measurements (25,26). The binding mode depends on the force applied on the DNA (26), the ionic conditions, the concentration of SSB and ssDNA (23), and the configuration of the C-terminal tails (14,26–28). The C-terminal tails are essential, as deleting the last 10 amino acids is lethal in *E. coli* (29). Moreover, several DNA-processing enzymes specifically interact with the last 4–9 residues (C-terminal peptide, CTP) of the C-terminal tail (6,9,17). This interaction has been shown to stimulate the activity of RecQ and other proteins (5–7,9), but it is unclear if this stimulation results from enhanced binding via SSB recruitment, or *bona fide* stimulation of enzyme catalysis through interaction with the SSB CTP.

RecQ-family helicases are conserved from *E. coli* to humans (30–32). These enzymes catalyze strand separation of double-stranded (ds) DNA coupled to ATP hydrolysis (30–33). They are involved in the resolution of complex DNA structures such as double-Holliday junctions, displacement (D-) loops, and converging replication forks (30–32,34–37). Mutations of the human RecQ helicases, WRN, BLM and

*To whom correspondence should be addressed. Tel: +1 301 480 4076; Fax: +1 301 402 3404; Email: neumankc@mail.nih.gov
Correspondence may also be addressed to Mihály Kovács. Email: mihaly.kovacs@ttk.elte.hu
†These authors contributed equally to this work as first authors.

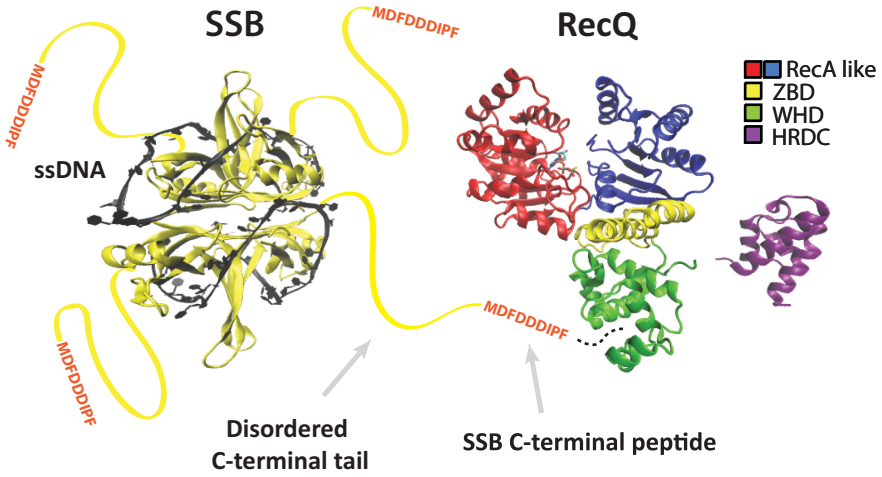

Figure 1. Physical and functional interactions between RecQ and SSB. Crystal structure of the *E. coli* SSB homotetramer (yellow) bound to two 35-mer ssDNA molecules (gray) (PDB ID: 1EYG). The unstructured C-terminal tails of SSB are represented with yellow lines and the amino acid sequence of the terminal 9 residues in red (C-Terminal peptide, CTP). Dashed line indicates the location of the interaction with the winged helix domain of *E. coli* RecQ (core PDB ID: 1OYY, HRDC PDB ID: 1WUD). Individual domains of RecQ are color coded as shown: zinc binding domain (ZBD), winged helix domain (WHD) and helicase and RNAse-D C-terminal domain (HRDC). ATPγS (stick model) is bound in the ATP binding site in the motor core.

RecQ4, have been linked to genetic disorders characterized by premature aging and cancer (32,38,39).

Many RecQ helicases share a conserved domain architecture of two RecA-like helicase domains (H1 and H2), a zinc-finger domain, a winged-helix domain (WHD), and a helicase and RNaseD C-terminal domain (HRDC) (Figure 1) (35,36,40,41). The RecA-like domains are responsible for ATP hydrolysis and ssDNA translocation, whereas the WHD and HRDC domains are involved in duplex and single-stranded DNA interactions, respectively (41–45). RecQ helicases physically interact with ssDNA-binding proteins: SSB in prokaryotes and Replication Protein A (RPA) in eukaryotes (46–49). Recent studies indicate that SSB enhances RecQ's unwinding activity via direct interaction between RecQ WHD and the C-terminal peptide (CTP) of SSB (7,17). Accordingly, the deletion of the CTP from SSB (SSBdC) has an inhibitory effect on the DNA binding and unwinding activity of RecQ, suggesting that in the absence of the interaction SSB blocks access of RecQ to DNA (7). *In vivo* studies in *Bacillus subtilis* showed that SSB recruits RecQ and other DNA repair proteins to stalled replication forks via the interactions of its CTP (8,10). These results indicate an important physiological role for RecQ–SSB interactions. Yet, the questions remain how the interactions with the SSB CTP allows RecQ to displace SSB to gain access to ssDNA, and how these interactions stimulate RecQ activity. Is it due only to recruitment of RecQ to ssDNA by SSB and stabilization of newly unwound DNA by SSB as proposed (7), or does the interaction stimulate RecQ catalytic activity?

Here, through a combination of single-molecule, biochemical, and rapid kinetic experiments, we elucidate a mechanism by which RecQ binding to the C-terminal peptide of SSB induces a dynamic structural transition from an SSB–DNA complex to a RecQ–SSB–DNA ternary complex. Importantly, our results reveal a RecQ-induced conversion of the SSB–ssDNA complex that results in the displacement of SSB. Ultimately, this mechanism affords RecQ access to SSB-bound ssDNA, which is critical for initiation of its DNA-restructuring activities. Our results support a general model in which the SSB CTP serves both as a hub that recruits DNA metabolic enzymes and, at the same time, a switch that mediates partner-induced changes in the DNA binding properties of SSB to regulate access to DNA. Furthermore, our results show directly that this interaction increases the on-rate of RecQ and modestly enhances its unwinding activity. Taken together these results suggest a reciprocal interaction in which each protein modulates the behavior of the other.

MATERIALS AND METHODS

Reagents

All reagents were from Sigma-Aldrich unless otherwise stated. ATP was from Roche Applied Science. MDCC (7-diethylamino-3-((((2-maleimidyl)ethyl)amino)carbonyl)coumarin) was from Life Technologies. For concentration determination, ϵ_{260} values of 8400 M^{-1} cm^{-1} nt^{-1} and 10 300 M^{-1} cm^{-1} nt^{-1} were used for oligo-dT and for non-homopolymeric oligonucleotides, respectively. DNA concentrations are expressed as those of oligo- or polynucleotide molecules (as opposed to those of constituent nucleotide units (nt)) unless otherwise stated.

Protein preparation and peptides

RecQ and RecQdWH were prepared as in (50,51). RecQdH was prepared as in (52). SSB, SSBdC and SSB-G26C were prepared as in (53) and (54), respectively. Labeling of SSB-G26C with MDCC was performed as in (55). SSB concentrations are given in tetramers if not indicated otherwise.

Unlabeled peptides were from Life Technologies. C9-FLU was from LifeTein. Peptides were dissolved in 20 mM Tris pH 7.5, 50 mM NaCl, 20 mM ammonium bicarbonate.

Proteins and peptides used in this study are described in Supplementary Table S1.

DNA constructs

Hairpin DNA constructs for magnetic tweezers experiments were prepared as described as in (52). For the hairpin refolding assay, we generated a 537-base hairpin with ds-DNA handles on both ends. The top handle was modified with biotin on the 3′ end for attachment to a streptavidin coated magnetic bead and the bottom handle was modified with three digoxigenin at the 5′ end for attachment to the coverslip. For helicase assays, we generated a 584-base hairpin with a 1.1 kB dsDNA handle on the 5′ end and a dT_{54} ssDNA region on the 3′ end. The handle was modified with three digoxigenin at the 5′ end and the dT_{54} was labeled on the 3′ end with biotin. Oligonucleotides for hairpin generation were purchased from Operon.

Magnetic tweezers sample cell preparation

The single-molecule helicase assay is described in detail in (52). Briefly, 5–10 × 10^{-15} mol DNA substrate was mixed with ∼100 ng anti-digoxygenin antibody and incubated in a sample cell overnight at 4°C. Unbound DNA was washed out with 200 μl of wash buffer (PBS supplemented with 0.04% v/v Tween-20 and 0.3% w/v BSA). 1-μm streptavidin-coated magnetic beads (MyOne, Invitrogen) were introduced into the sample cell and allowed to bind DNA for 5 minutes. The sample cell was then washed with 1 ml wash buffer. Measurements were taken at room temperature on a commercial Picotwist instrument. Bead position in three dimensions was acquired at 60 Hz.

Magnetic tweezers competition experiments

RecQdH, SSB, or SSBdC was diluted to 500 nM in 50 mM reaction buffer (50 mM Tris–HCl (pH 8.0), 30 mM monopotassium L-glutamic acid, 1 mM Mg L-glutamic acid, 0.1% Tween, 0.03% BSA, 1 mM DTT) and introduced into the sample cell. In competition experiments, 500 nM SSB or SSBdC was mixed with 250 nM RecQdH. A force of 17 pN was applied to mechanically unfold the DNA hairpin and protein was allowed to bind the ssDNA for 5–10 s. The force was then lowered to 8 pN. This force is below the critical unfolding force of the DNA hairpin, but is sufficient to reduce thermal fluctuations. Once the hairpin had returned to the folded state, the DNA was unfolded again and the measurement repeated.

Magnetic tweezers helicase experiments

For helicase assays, RecQdH was incubated with SSB constructs at a concentration of 1.5 μM each for 30 minutes at room temperature. RecQ/RecQdH alone or mixed 1-to-1 with SSB constructs was diluted to 50 pM in reaction buffer with 1 mM ATP and introduced to the sample cell. The chamber was then washed with 200 μl reaction buffer with 50 mM potassium glutamate. A force of 8 pN was applied on the DNA hairpin. This force results in an increase in the height of the magnetic bead of ∼0.8 nm per base pair of hairpin unwound.

Fluorescence intensity titrations

Unless stated otherwise, all ensemble measurements were performed at 25°C in SF50 buffer (50 mM Tris–HCl pH 7.5, 50 mM NaCl, 1 mM DTT, 5 mM $MgCl_2$, 50 μg/ml BSA). SF200 buffer is as SF50 buffer but contains 200 mM NaCl. Fluorescence intensity measurements were carried out in a SPEX Fluoromax spectrofluorometer. DCC-SSB was excited at 436 nm (1-nm bandwidth), and the fluorescence emission spectrum (450–550 nm, 4-nm bandwidth) of each titration point was recorded.

Fluorescence anisotropy titrations

In C9-Flu binding experiments, 15 nM of C9-Flu was titrated with increasing concentrations of protein. In competitive titration experiments, unlabeled C9 was used to compete with C9-Flu for binding to RecQ constructs. Fluorescence anisotropy was measured in a Synergy H4 Hybrid Multi-Mode Microplate Reader (BioTek).

ATPase measurements

Steady-state ATPase activities were measured by using a pyruvate kinase-lactate dehydrogenase (PK-LDH) coupled assay (14 U/ml PK, 20 U/ml LDH, 1 mM ATP, 1 mM phosphoenol pyruvate, 200 μM NADH). Time courses of NADH absorbance ($\epsilon_{340} = 6220\ M^{-1}\ cm^{-1}$) were followed in a Shimadzu UV-2101PC spectrophotometer.

Stopped-flow measurements

Stopped-flow measurements were carried out in a Bio-Logic SFM 300 instrument. Post-mixing concentrations are stated. DCC-SSB fluorescence was monitored as in (55).

Data analysis

Means ± SEM values are reported unless otherwise specified. Data analysis for ensemble assays was performed using OriginLab 8.0 (Microcal corp.). For magnetic tweezers experiments, data analysis was performed using Igor Pro 6.3A. Helicase kinetics were extracted using a *t*-test based step-finder (52). Global kinetic fitting was performed using KinTek Global Kinetic Explorer 4.0 (56).

RESULTS

Binding of RecQ to SSB triggers SSB displacement from DNA

We probed the interactions of RecQ and SSB with ssDNA by measuring the effect of the proteins on the refolding of a 537-bp DNA hairpin in magnetic tweezers experiments (Figure 2A). The hairpin was attached to a glass coverslip and a magnetic bead via dsDNA handles labeled with biotin on one end and digoxygenin on the other (52). A pair of magnets above the sample chamber was used to apply force on the DNA substrate via the magnetic bead. At a force of 8 pN the DNA hairpin remains folded but is unfolded at a force of 17 pN (Figure 2A and B). The experiments consisted of switching between the force to unfold

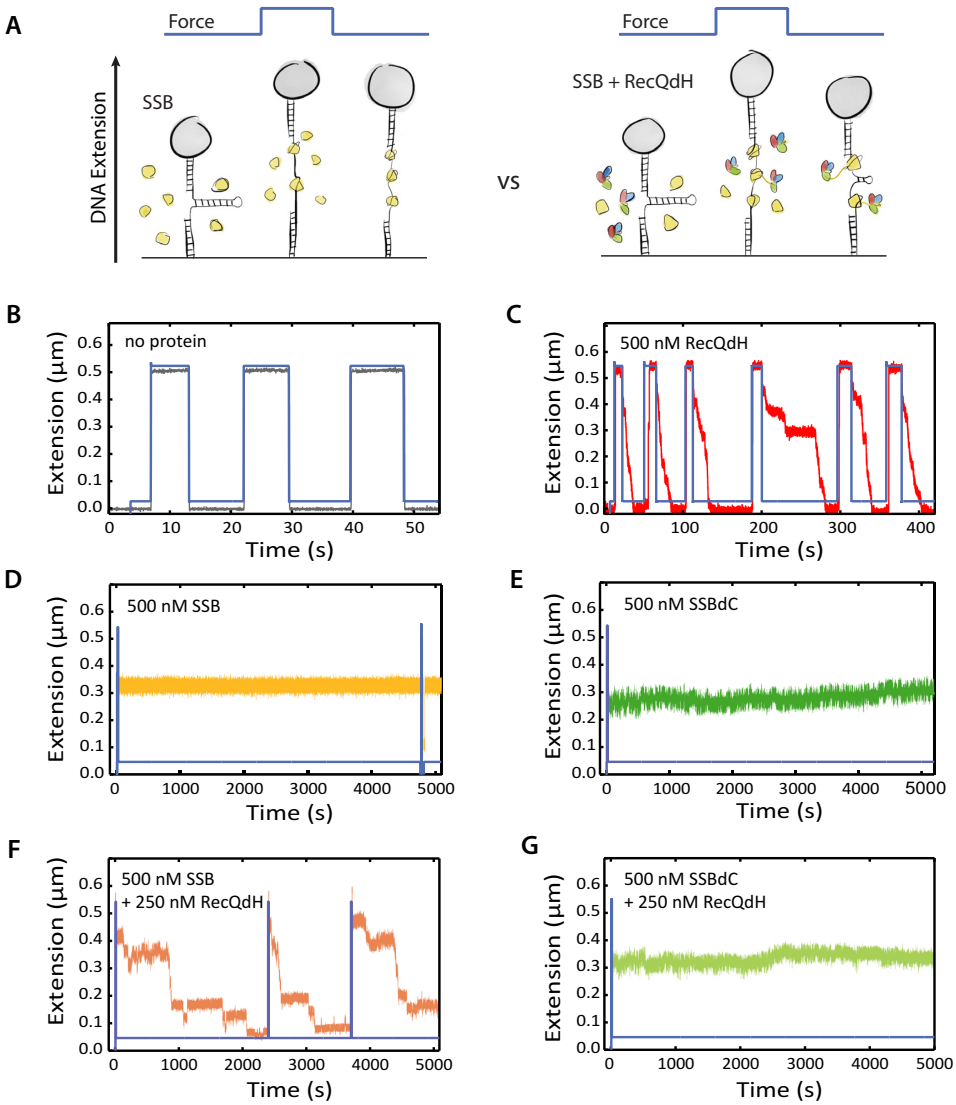

Figure 2. RecQ–SSB interaction destabilizes SSB–ssDNA binding. (**A**) Magnetic tweezers-based ssDNA interaction assay. A 537-bp DNA hairpin is unfolded and refolded by modulating the force in the presence or absence of proteins (color coded as in Figure 1). Sequestration of ssDNA by bound protein is detected as a delay or failure of hairpin refolding at low force. (B–G) Mechanical DNA hairpin unfolding and refolding traces recorded in the presence of: (**B**) no protein, (**C**) 500 nM RecQdH, (**D**) 500 nM SSB, (**E**) 500 nM SSBdC, (**F**) 500 nM SSB plus 250 nM RecQdH and (**G**) 500 nM SSBdC plus 250 nM RecQdH (ATP was absent in all experiments). Note the different time-scales. Blue lines represent the applied force.

and refold the hairpin in the presence or absence of RecQ and SSB constructs. We used a HRDC-deletion RecQ construct (RecQdH) (Supplementary Table S1) that exhibits simpler DNA hairpin unwinding kinetics than wild-type (WT) RecQ, while retaining its DNA and SSB-interacting properties (42,43). All of the hairpin unfolding and refolding experiments were performed in the absence of ATP so the results are not dependent on translocation of RecQ on the DNA. In the presence of RecQdH (500 nM) the DNA hairpin slowly refolded in multiple steps of variable duration and extension change, requiring 20–100 s to completely refold. This indicates that slow release of individual RecQ molecules bound to ssDNA impedes reformation of the hairpin after the force is reduced (Figure 2C). In the presence of 500 nM SSB, the hairpin remained open indefinitely (>5000 s) after the force was decreased, indicating stable binding of SSB (Figure 2D). The same was true of the SSBdC construct lacking the last eight residues of WT SSB corresponding to the C-terminal peptide (Figure 2E, Supplementary Table S1). Whereas the average DNA extension was constant after reducing the force, discrete fluctuations were observed in the presence of SSBdC. This is consistent with previous evidence indicating that deletion of the CTP affects the affinity of SSB for ssDNA and the preference for the 35-nt binding mode by influencing the binding mode transition rates (25,57).

The inhibition of hairpin refolding by SSB and SSBdC indicates very low ssDNA dissociation rates. Importantly, however, when 250 nM RecQdH and 500 nM SSB were added together, the hairpin no longer remained open at low force but gradually refolded, indicating that RecQdH induced the displacement of SSB molecules from ssDNA

(Figure 2F). The lower concentration of RecQdH as well as the lower affinity of RecQdH for ssDNA (Figure 2C) makes it unlikely that this refolding results from RecQdH displacing SSB through simple competition. The refolding happened in multiple steps and was accompanied by fluctuations in DNA extension that were not apparent in the absence of RecQdH. RecQdH did not have any effect on SSBdC bound to the unfolded hairpin, despite the potentially increased inherent dissociation rate of SSBdC compared to SSB, demonstrating that a direct interaction between RecQ and SSB, mediated by the CTP, is required for RecQ-induced SSB removal from ssDNA (Figure 2G). These results show that the binding of RecQ to the SSB CTP destabilizes the SSB–ssDNA complex in a way that enables RecQ to access the DNA.

To determine the magnitude of the fluctuations observed in the SSBdC and SSB + RecQdH experiments, extension traces for SSB, SSBdC and SSB + RecQdH were smoothed with a Savitzky-Golay filter and histogrammed (Figure 3A, Supplementary Table S2). The histogram values were adjusted so that the dominant peak corresponded to zero and then fit with single or multiple Gaussians. For multi-Gaussian fits, the standard deviation for all peaks was fixed at a value representing the inherent noise in the measurement whereas means and amplitudes were unconstrained. To separate fluctuations from SSB displacement in the SSB + RecQdH data, histograms were collected for each observed plateau and then combined. In the presence of SSB, no fluctuations in extension above noise were detected (Figure 3A-B, Supplementary Table S2). For SSBdC, however, distinct peaks were observed. Multiple Gaussian fits of these peaks are consistent with changes in DNA extension on the order of 35 and 65-nt occurring every 5–20 seconds (Figure 3A-B, Supplementary Table S2). The fluctuations were smaller overall in the SSB + RecQdH system (Figure 3A-B, Supplementary Table S2). The noise in the SSB + RecQdH data is also lower than in the other systems, allowing detection of smaller changes. The lower noise is a reflection of the decrease in the extension of the ssDNA, as the hairpin refolds during these experiments. In contrast to the SSBdC results, a multiple Gaussian fit of the SSB + RecQdH data yields peaks very close to known SSB binding modes of 17, 35, and 56 nt (Figure 3A-B, Supplementary Table S2) (21,25,26). These results suggest that RecQ not only displaces SSB, but does so by changing the SSB–DNA binding mode.

RecQ elicits a change in the DNA binding mode of SSB to gain access to ssDNA

To determine whether RecQ can displace SSB from ssDNA in the absence of the assisting force of hairpin refolding, we utilized a well-characterized fluorescently labeled SSB construct (DCC-SSB) (Supplementary Figure S1) (54,58). Fluorescence emission of DCC-SSB increases ∼6 fold upon binding ssDNA (Supplementary Figure S1A). The fluorescence emission of DCC-SSB is also sensitive to the ssDNA binding mode (Supplementary Figure S1) (54,58).

In competitive equilibrium titration experiments, 50 nM DCC-SSB was preincubated with 50 nM dT_{72} and then mixed with various RecQ concentrations in SF50 buffer, containing intermediate concentrations of salts (50 mM NaCl and 5 mM $MgCl_2$). Under these conditions, SSB binds to dT_{72} with 1:1 stoichiometry (Supplementary Figure S1) in the 65 nt binding mode (54,58) in the absence of RecQ. Increasing RecQ concentrations suppressed DCC-SSB fluorescence to about half of the RecQ-free level (Figure 4A, Supplementary Table S3). The reduced DCC-SSB fluorescence level may reflect either a simple competition between RecQ and DCC-SSB for ssDNA binding, or the formation of a RecQ.DCC–SSB.ssDNA ternary complex with decreased fluorescence compared to that of DCC-SSB.ssDNA alone. The amplitude of the fluorescence change was significantly suppressed by the inclusion of 50 μM of a nine residue SSB CTP mimic peptide (C9, Supplementary Table S1) (Figure 4A), in agreement with the results of the magnetic tweezers experiments (Figure 2F and G).

To resolve the mechanism underlying the RecQ-induced change in DCC-SSB fluorescence, we measured the kinetics of the fluorescence change upon rapidly mixing 50 nM DCC-SSB and 50 nM dT_{72} with various concentrations of RecQ in a stopped-flow instrument. In buffers containing intermediate (SF50, Figure 4B) or high concentrations of salts (SF200, Supplementary Figure S2B), SSB binds to dT_{72} with 1:1 stoichiometry in the 65 nt binding mode (54,58) in the absence of RecQ.

Traces showed complex multiphasic behavior, indicative of multiple kinetic steps. In SF50 buffer, a rapid exponential phase was observed along with a complex slow phase. The observed rate constant (k_{obs}) of the rapid phase showed saturation with increasing RecQ concentration (Supplementary Figure S2A). In the presence of 50 μM C9 peptide, the amplitude of the traces and the rapid-phase k_{obs} values were suppressed (Supplementary Figure S2C). Kinetic modeling revealed that a simple competition model cannot account for the observed behavior (Supplementary Figure S2D–F). Therefore, we developed a kinetic model that takes into account all plausible interactions among SSB, RecQ and ssDNA that are supported by our and others' observations (Figure 5).

In our model (Figure 5) one DCC-SSB molecule can rapidly bind (cf. Supplementary Figure S1B and C) to dT_{72} in the 65-nt binding mode (SSB**.dT_{72}, with ∼6 times enhanced fluorescence level compared to free DCC-SSB; cf. Supplementary Figure S1A) (step (*i*) in the scheme). Dissociation of SSB from ssDNA in the 65-nt binding mode is very slow (cf. Supplementary Figure S1F). The 65-nt complex can transition into the 35-nt mode (SSB*.dT_{72}) (25) (*ii*); however, in the measurement buffer conditions, the equilibrium is shifted toward the 65 nt binding mode (Supplementary Figure S1A). Based on the results of Supplementary Figure S1D and Kunzelmann *et al.* (58), the fluorescence level of DCC-SSB in the 35-nt binding mode is ∼0.4 that in the 65-nt binding mode.

RecQ competes with SSB for binding to free dT_{72}. Previously the binding site size of RecQ was determined via different methods and under different conditions to range from 9 to 33 nt (33,42,43,50,59–61) with a mean of ∼18 nts. We therefore considered that 2–7 RecQ molecules can bind to a dT_{72} molecule in consecutive steps, forming $RecQ_n$.dT_{72} complexes (*iii–vi*). Best fits of the slow complex

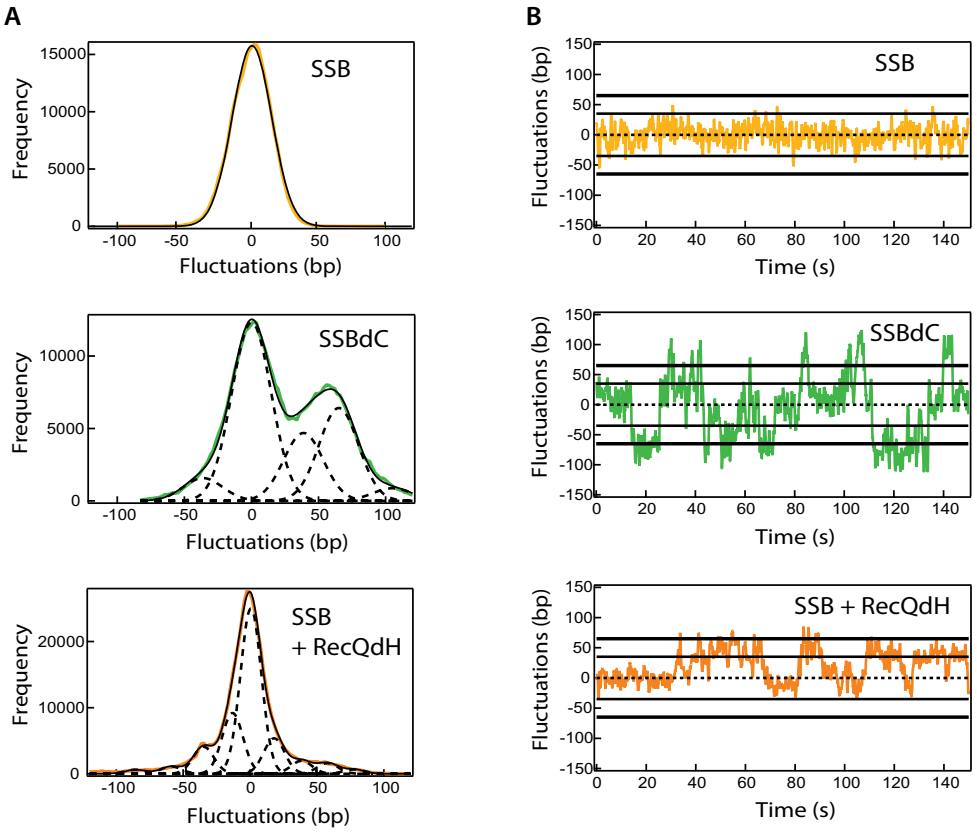

Figure 3. RecQ modulates the binding mode of SSB. (**A**) Histograms of DNA extension fluctuations from hairpin refolding measurements in Figure 2. Dashed lines indicate individual peaks from multi-Gaussian fits. Solid black lines represent the combined multi-Gaussian fit. The dominant peak in each histogram was set to 0. The SSB data was fit with a single Gaussian with x0 = 0 bp and $\sigma = 14.7 \pm 0.1$ bp. The standard deviation of the SSB data represents the baseline noise in the measurements that is expected to remain constant and uniform. We therefore fixed the standard deviation of the Gaussian distributions in the fits of the fluctuation histograms. Fitting the SSBdC data with multiple Gaussians with standard deviation of 14.7 bp returned mean values of -36.2 ± 0.1, 0, 38.6 ± 0.2, 64.9 ± 0.1, and 105.0 ± 0.2 bp. Fitting the SSB + RecQdH data with multiple Gaussians with standard deviation of 7.7 bp returned mean values of -86.1 ± 0.1, -59.6 ± 0.1, -35.4 ± 0.0, -13.7 ± 0.1, 0, 17.4 ± 0.1, 37.8 ± 0.2, 57.4 ± 0.1, and 77.2 ± 0.1 bp. (**B**) Examples of fluctuations for SSB, SSBdC, and SSB + RecQdH over 150 s of data traces with a dashed black line at 0 and solid black lines at -65, -35, 35, and 65. The results of the multi-Gaussian fitting are presented in Supplementary Table S2.

kinetic behavior were obtained with four consecutive binding steps, suggesting that the binding site of RecQ is close to the 18 nt mean value, consistent with the 18 ± 2 nt value determined by us previously (50).

RecQ can also bind to the SSB**.dT_{72} complex (65-nt binding mode, moderate RecQ affinity), possibly mediated by interaction with the CTP of SSB, to form the RecQ.SSB**.dT_{72} ternary complex (*vii*) (Figure 5). Interaction of RecQ with SSB can shift the equilibrium from the 65-nt to the 35-nt binding mode, and thus can lead to the formation of RecQ.SSB*.dT_{72} (*viii*). This model, involving RecQ binding-induced 65-nt to 35-nt conversion, is supported by the findings that the observed rate constant of the first phase observed in SF50 buffer (a) depends on RecQ concentration and saturates at high RecQ concentrations (Supplementary Figure S2A), (b) is much faster than the dissociation rate constant of SSB from ssDNA (Supplementary Figure S1), and (*c*) the observed rate constant at saturating RecQ concentration is similar to the observed rate constants of the rapid phase observed in DCC-SSB dissociation experiments with saturating unlabeled SSB (Supplementary Figure S1D-E). The RecQ.SSB*.dT_{72} ternary complex can also form if a RecQ molecule binds to SSB*.dT_{72} (*ix*) or SSB binds to RecQ.dT_{72} (*x*). However, these steps occur rarely due to the low amount of SSB*.dT_{72} and free SSB. Either RecQ (*ix*) or SSB (*x*) can dissociate from the RecQ.SSB*.dT_{72} ternary complex. For maximal reasonable simplification of the model, we considered binding of RecQ to SSB to occur with a 1:1 stoichiometry. Since four CTP are present on an SSB tetramer, we cannot rule out more complicated scenarios of multiple (up to 4) RecQ molecules binding to an SSB tetramer. SSB* and RecQ together may occlude about 53 (35 + 18) nt and leave 19 nt unbound in dT_{72}. Given this, it is conceivable that another RecQ molecule is able bind to the ternary complex, thus forming $RecQ_2$.SSB*.dT_{72} (*xii*). The same complex can alternatively form via binding of SSB to $RecQ_2$.dT_{72} (*xiii*). From this complex, either SSB (*xiii*) or RecQ (*xii*) can dissociate.

Elimination of any of the above steps significantly deteriorated the quality of the fits. During fitting, rate constants colored black were fixed (Figure 5). Rate constants with the same color were floated in parallel (i.e. their ratios were kept fixed). Determined parameters are listed in Supplementary

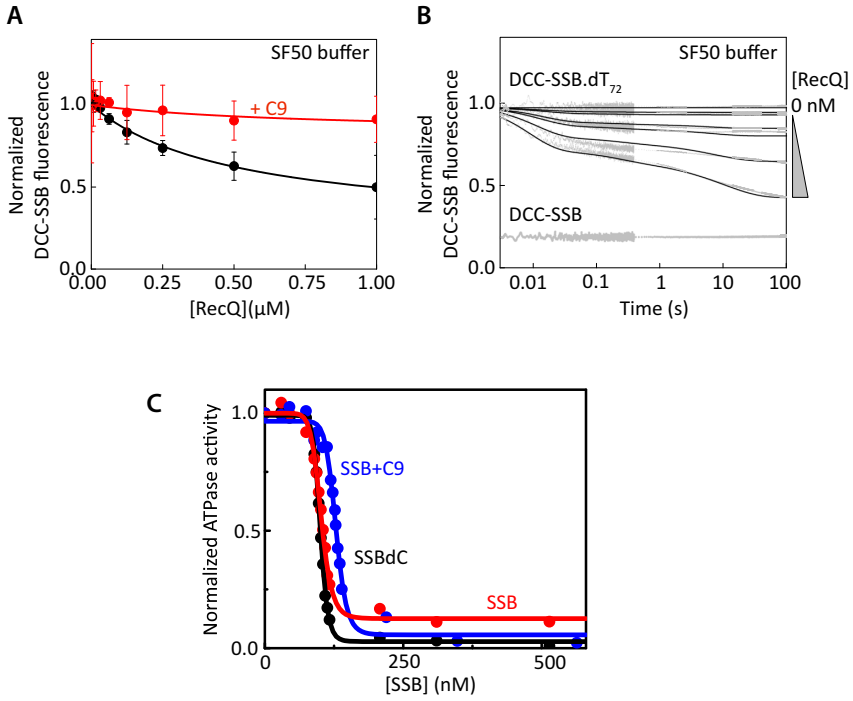

Figure 4. RecQ induces a binding mode change in the SSB.ssDNA complex. (**A**) Equilibrium fluorescence titrations of 50 nM fluorescently labeled (DCC-) SSB and 50 nM dT_{72} with increasing concentrations of RecQ in the absence of MgATP without (black) or with C9 peptide (50 μM, red) in SF50 buffer. Fluorescence levels are normalized to that of DCC-SSB in the absence of RecQ. Lines show hyperbolic fits. Determined parameters are listed in Supplementary Table S3. (**B**) Stopped-flow time courses of DCC-SSB fluorescence change upon rapidly mixing 50 nM DCC-SSB and 50 nM dT_{72} with different concentrations of RecQ from 0 to 1200 nM (no ATP present) in SF50 buffer (50 mM NaCl, 5 mM $MgCl_2$). (See Supplementary Figure S2B for data recorded in SF200 buffer.) RecQ concentrations from top to bottom are 0, 50, 100, 200, 300, 600 and 1200 nM. Solid lines show best fits based on the model shown in Figure 5. Determined parameters are listed in Supplementary Table S4. (**C**) Comparison of the effect of SSB (red symbols) and SSBdC (black symbols), and SSB + C9 (blue symbols) on the dT_{54} (100 nM) activated ATPase activity of RecQ (15 nM). ATPase values are normalized to that of RecQ in the presence of dT_{54} without SSB.

Table S4. An alternative model, involving the assumption that a fraction of DNA-bound SSB has a very short lifetime, failed to reproduce the observed kinetic behavior, especially the rapid phase of the traces.

In addition to the above conclusions, the model suggests that, in SF200 buffer, the increased salt concentration slows down the 65-nt–35-nt mode transition, in line with the previous finding that the 65-nt mode is stabilized by increased NaCl concentrations (25). The increased salt concentration also slightly (∼2-fold) reduces the affinity of RecQ to SSB (Supplementary Table S4, see also Supplementary Figure S4A and C). Due to these effects, the rapid phase is not observable in SF200 buffer (Supplementary Figure S2B). The slowing of the 65-nt–35-nt mode transition by elevated salt concentration was further supported by our control experiments using unlabeled SSB instead of RecQ (Supplementary Figure S1E).

Importantly, our model can predict the concentration of different complexes under conditions expected in *Escherichia coli* cells, i.e. low RecQ/SSB molar ratios (3). Our model predicts that, even at high SSB concentrations, a significant number of RecQ.SSB.ssDNA ternary complexes will form (Supplementary Figure S3), due to the RecQ-CTP interaction (Supplementary Figure S4). To test this prediction, we performed ATPase activity measurements in which 15 nM RecQ was mixed with 100 nM dT_{54} and titrated with WT SSB or SSBdC. We used dT_{54} instead of dT_{72} to decrease the probability of two SSB tetramers binding to the same DNA molecule at high SSB concentrations. Saturating dT_{54} with SSB inhibited RecQ ATPase activity (Figure 4C). However, the ATPase activity was not suppressed to the DNA-free level (∼0.2 s^{-1}) (42,50) at high SSB concentrations but remained constant at an intermediate level (around 3 s^{-1}) (Figure 4C), as found previously (35,62). This characteristic 'residual' ATPase activity was not observed when SSB was replaced with SSBdC (Figure 4C). Here, RecQ ATPase activity was suppressed to the DNA-free level as the ternary complex does not form in the absence of the RecQ–SSB CTP interaction. The CTP-mediated formation of the ternary complex was further verified by the addition of isolated C9 peptide. Competition by C9 suppressed the residual RecQ ATPase activity in the presence of SSB below the level measured with SSBdC (Figure 4C and Supplementary Figure S3B).

SSB recruits RecQ to DNA and stimulates unwinding via interactions with the CTP

The above experiments revealed that, via an interaction with the SSB CTP, RecQ can form a ternary complex with SSB and ssDNA, thereby facilitating a binding mode transition in SSB and inducing SSB dissociation from ssDNA. We next assessed if the interaction with SSB influences ATP-dependent dsDNA unwinding activity by RecQ using

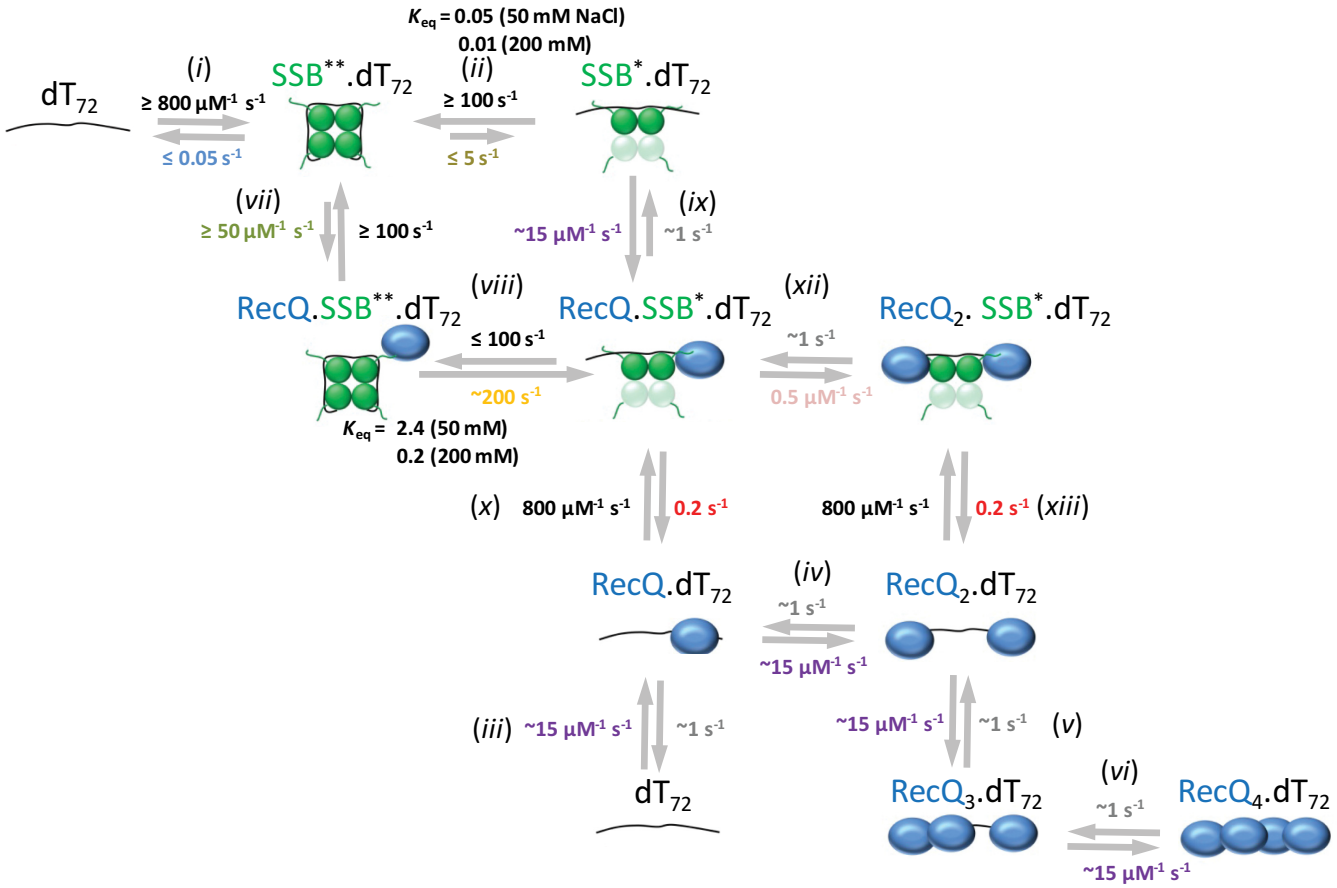

Figure 5. Kinetic model of RecQ.SSB.DNA interactions. Traces of Figure 4B and Supplementary Figure S2B contained multiple phases that could not be well fit by exponentials, suggesting multiple steps in the process and the lack of dominant rate-limiting step(s). Accordingly, simple models (Supplementary Figure S2D–F) were unable to reproduce the observed traces. This panel shows the minimal kinetic model that can reasonably account for the experimental results (steps of the model are described in the main text). Black lines represent ssDNA. Dark green, light green and blue cartoons represent ssDNA-bound DCC-SSB and ssDNA-free DCC-SSB and RecQ monomers, respectively. In the 65-nt binding mode (SSB**) all four SSB subunits interact with ssDNA; in the 35-nt mode (SSB*), on average two SSB subunits interact with ssDNA. The scheme is not intended to specify which monomers of the DCC-SSB tetramers are in contact with ssDNA in the different binding modes. Both in SF50 and SF200 buffers the equilibrium is shifted toward the SSB** mode in the absence of RecQ (cf. Supplementary Figure S1A). The increased salt concentration in SF200 buffer leads to even higher stabilization of the 65-nt binding mode. The RecQ–SSB interaction induces a rapid shift toward the SSB* (35-nt) mode. Rate constants obtained in SF50 buffer are indicated in the figure. All determined parameters are listed in Supplementary Table S4.

a magnetic tweezers-based hairpin DNA unwinding assay (43,52,63). In this assay, we measured the unwinding activity of individual RecQ helicase molecules with and without SSB on a 584 bp DNA hairpin that includes a 60-nt 3′ssDNA region adjacent to the ssDNA–dsDNA junction of the hairpin for RecQ to bind and initiate unwinding (Figure 6A). A force of 8 pN was applied to the DNA hairpin to reduce the measurement noise without opening the hairpin. Unwinding of the hairpin was measured via the increase in the extension of the DNA, which can be directly related to the number of base pairs (bp) unwound (Figure 6A) (52). This experimental design, in which the hairpin has a single ssDNA–dsDNA junction, along with a low RecQ concentration (50 pM), helps ensure that measurements correspond to the activity of a single RecQ helicase (43). Our previous studies of RecQ unwinding activity revealed that the HRDC domain contributes to extensive pausing and repetitive unwinding and reannealing of the DNA hairpin, which makes it difficult to measure the core helicase activity of the enzyme (43,52) (Supplementary Figure S5A). We therefore conducted our experiments with RecQdH (Supplementary Table S1) (7). We performed hairpin DNA unwinding experiments with RecQdH alone and in the presence of 50 pM WT SSB or 50 pM SSBdC. The low SSB concentrations minimize the probability of SSB–ssDNA binding, thus changes in unwinding activity are likely indicative of SSB–RecQ interactions.

Effects of SSB on the initiation of DNA unwinding by RecQ can be quantified from the mean time between unwinding events (T_{wait}) in the DNA unwinding trajectories (Figure 6B). We observed a roughly two-fold decrease in T_{wait}, from 262 ± 57 ms to 129 ± 26 ms in the presence of SSB, indicating that SSB promotes the initiation of RecQ DNA unwinding (Figure 6B-C, Supplementary Figure S5, Table S5). In contrast to the SSB effect, the presence of SSBdC did not change T_{wait} (255 ± 33). It is noteworthy that SSBdC did not hinder initiation of RecQ unwinding in our experiments (Figure 6D). As SSBdC has been shown to favor the 35-nt binding mode at the low salt concentration (57), the binding of an SSBdC tetramer to the 60-nt

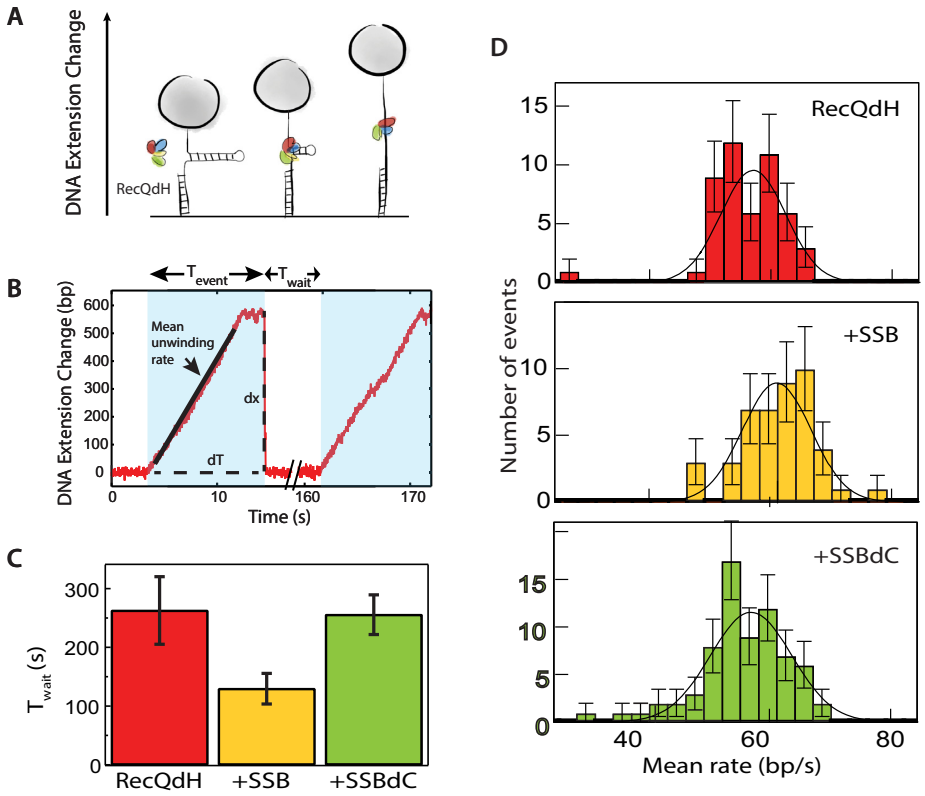

Figure 6. SSB stimulates RecQ binding to ssDNA and helicase activity via the CTP interaction. (**A**) Magnetic tweezers helicase hairpin unwinding assay. Extension of a 584-bp DNA hairpin is monitored as a function of time in the presence of RecQdH by measuring the position of a magnetic bead attached to one end of the DNA held at a constant force of 8 pN. (**B**) Illustration of magnetic tweezers data analysis. For each unwinding event, the mean unwinding rate, event duration, and time between events was characterized. (**C**) Average time between events (T_{wait}), determined from single exponential fits to the distribution of wait-times of RecQdH (262 ± 57 s), RecQdH +SSB (129 ± 26 s), and RecQdH +SSBdC (255 ± 33 s). (**D**) Histograms of mean unwinding rates from magnetic tweezers experiments. Solid lines are Gaussian fits. RecQdH x0 from fit = 56.0 ± 1.0 bp/s, RecQdH +SSB x0 = 60.2 ± 1.1 bp/s, RecQdH + SSBdC x0 = 55.6 ± 1.1 bp/s.

ssDNA loading site on the hairpin DNA substrate likely leaves enough exposed ssDNA for RecQ binding and unwinding initiation.

To determine whether SSB directly effects RecQ unwinding, we analyzed the mean unwinding rates from the slopes of the unwinding trajectories (Figure 6B and D). We found that SSB increased the mean rate of unwinding from 56.0 ± 1.0 bp/s to 60.2 ± 1.1 bp/s (Figure 6D, Supplementary Table S5). While this increase is modest, on the order of 7%, it is noteworthy that this stimulation is present throughout unwinding traces. In contrast, SSBdC did not have a statistically significant effect on the mean unwinding rate (55.6 ± 1.1 bp/s). This suggests that the interaction with SSB impacts the unwinding activity of RecQ as well as RecQ–DNA binding.

DISCUSSION

SSB is known to both sequester and protect ssDNA (1–5) and stimulate the activity of DNA processing enzymes (5–7,9). During replication, SSB binds to nascent ssDNA and remains associated with it if the replication fork stalls either due to DNA lesions (8,10,64) or when the forks converge at the end of replication, forming a late replication intermediate (37). *Escherichia coli* RecQ participates in numerous processes of genome maintenance. In conjunction with SSB, RecQ is involved in resection of DNA double-strand breaks (65), in the formation and disruption of joint DNA molecules (66), in the rescue of stalled replication forks (64) and in the dissolution of late replication intermediates (37). It is still unknown which SSB binding mode is dominant in these situations, but all known modes may occur *in vivo* (67).

Recent evidence indicates that interactions between SSB and its partner proteins may change the SSB–DNA binding mode in such a way as to allow these proteins access to the DNA (13,68). In this study, we show that the behavior of SSB is altered by interaction of RecQ with the C-terminal tails, which elicits a rapid decrease in the ssDNA binding affinity of SSB in an ATP-independent manner (Figures 2 and 4). Our data also suggests that SSB recruits RecQ helicase to both ssDNA and ssDNA–dsDNA junctions by increasing the on-rate of RecQ, and that SSB stimulates the DNA unwinding rate of RecQ through the interaction with the C-terminal tail (CTP) (Figures 6 and 7, Supplementary Figure S6; Table S5) (43). These results support the idea that SSB acts as a complex-forming platform that marks DNA sites to which RecQ and other SSB-interacting proteins are recruited (69).

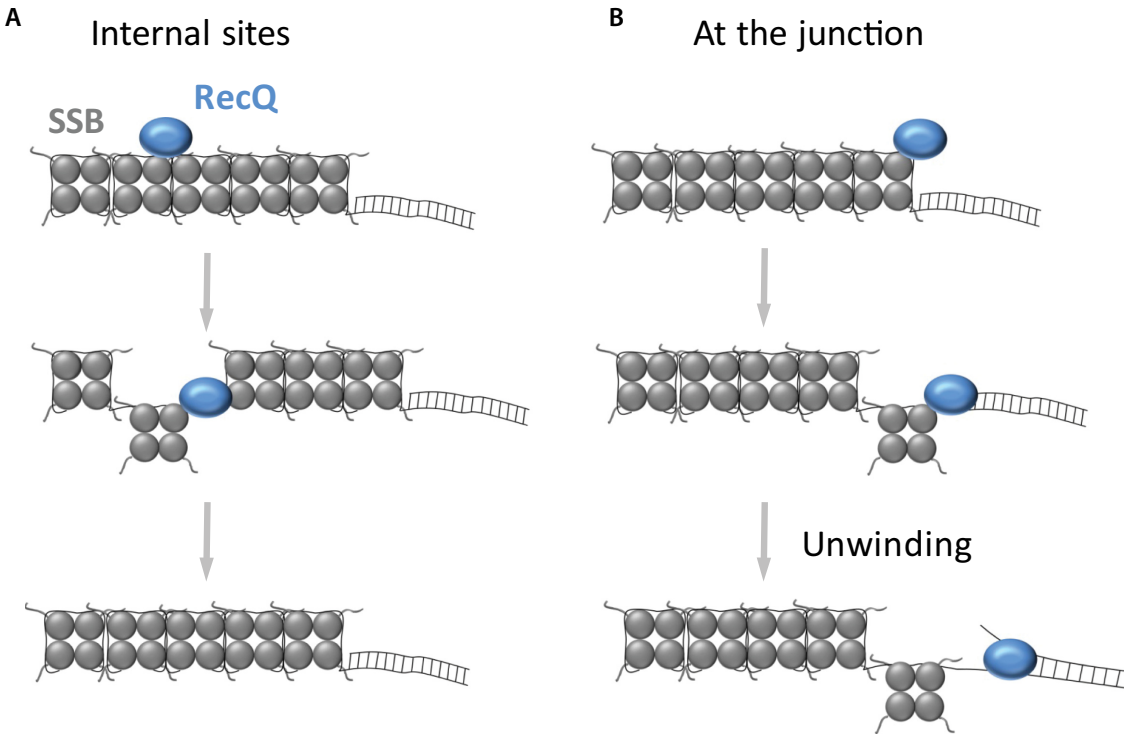

Figure 7. The RecQ–SSB interaction can efficiently steer the helicase to the ssDNA/dsDNA junction to initiate DNA unwinding. (**A**) Rapidly forming, short-lifetime interactions of RecQ with the SSB CTP enable rapid probing of the SSB–ssDNA filament at internal sites. (**B**) Formation of the RecQ.SSB.DNA ternary complex at an ssDNA–dsDNA junction will efficiently initiate DNA unwinding.

The C-terminal tail is known to affect the wrapping mode and cooperativity of the SSB–ssDNA interaction (27,28,57,70). Deletion of the C-terminal tail results in a preference for the 35-nt mode (57) and thus can increase the dissociation rate of the tetramer (25). Our results show that binding of the CTP by RecQ results in a similar destabilizing effect on SSB–ssDNA binding. We note that this destabilization was observed even at SSB:RecQ (tetramer:monomer) concentration ratios of 2:1 (Figure 2F) and 1:1 (Figure 4B). SSB is a homotetramer and, thus, in principle it could interact with as many as four RecQ molecules. Under our experimental conditions, only one or two RecQ molecules are expected to be bound to an SSB tetramer, indicating that the destabilization occurs even if a fraction of the CTPs are sequestered. This finding is consistent with previous results showing that the deletion of two or three of the four C-terminal tails of an SSB tetramer is sufficient to alter its binding mode preference (27). Similar to our findings with RecQ, the *E. coli* DNA replication restart proteins PriA and PriC have recently been shown to facilitate the conversion from the 65-nt to the 35-nt mode, mediated by interaction with the SSB C-terminal tail (13,68), whereas RecO has been shown to displace SSB (15).

The RecQ-induced SSB binding mode change may serve multiple purposes *in vivo.* Mechanistic roles can be envisaged for each binding mode based on available knowledge. One possibility is that *in vivo* SSB covers all available ssDNA, predominantly in the 65-nt mode. In this case, the rapidly forming, short-lifetime interactions of RecQ with the SSB C-terminal segments (Figure 5, Supplementary Table S4) allow the enzyme to rapidly probe the SSB–ssDNA filament via formation of transient ternary complexes in which both proteins bind to ssDNA. Ternary complexes formed at internal sites of an ssDNA segment will be short-lived as SSB molecules before and behind the helicase will inhibit translocation (Figure 7A). Importantly, however, the formation of the ternary complex at an ssDNA–dsDNA junction will lead to unwinding, thereby effectively steering RecQ to the site of action (Figure 7B).

Another possibility is that SSB is dominantly present in its 35-nt mode and forms compact ssDNA-SSB filaments, due to the known cooperativity of this mode (23). In this situation, only a small fraction of SSB tetramers, especially ones that are located at the ends of the SSB–ssDNA filament are able to adopt the 65-nt mode. In this case, the rapid interactions between RecQ and SSB serve to capture RecQ in the vicinity of the ss-dsDNA junction, without allowing access of RecQ to ssDNA at internal sites of the filament. On one hand, the short lifetime of the interaction prevents futile anchoring of RecQ to SSB at internal positions of the filament. On the other hand, the binding of RecQ to terminal SSB molecules in the 65-nt mode located at the ssDNA–dsDNA junction elicits the binding mode change of SSB and allows RecQ to gain access to ssDNA from which dsDNA unwinding can start.

In either of the above scenarios, the SSB CTP-mediated interactions serve to recruit RecQ or other DNA-modifying proteins specifically to their site of action, and provide access to ssDNA at ssDNA–dsDNA junctions. These mech-

anisms, along with the ability of SSB to diffuse on ssDNA in both the 65-nt and 35-nt modes (12,71) can explain how SSB allows localized recruitment of binding partners without inhibition of their activities, and why *E. coli* cells expressing SSB mutants that can form only either the 65-nt or 35-nt binding mode but possess an intact CTP are viable, whereas deletion of the CTP is lethal (27,67).

In addition, the binding mode conversion facilitates displacement of SSB from ssDNA. SSB alone dissociates very slowly from ssDNA (72). Dissociation is thought to proceed through a DNA unwrapping process in which SSB monomers lose contacts with ssDNA (26,71). In this context, a RecQ-induced 65-nt to 35-nt mode change and stabilization of the 35-nt mode likely facilitate SSB dissociation. Our transient kinetic results suggest that dissociation of SSB from the 35-nt mode is faster than that from the 65-nt mode in which ssDNA is fully wrapped around the tetramer (Figures 4 and 5, Supplementary Figure S1, Table S4).

The ability of RecQ to facilitate SSB displacement from ssDNA through interaction with the CTP is readily apparent in the DNA hairpin refolding experiments (Figures 2 and 3). Here, SSB dissociation is coupled to the energetically favorable reformation of dsDNA. SSB alone inhibits hairpin reformation; however, RecQ (which otherwise has a low ssDNA binding affinity compared to SSB) (51) accelerates SSB dissociation even in the absence of ATP. Importantly, this result underscores that, despite SSB's high ssDNA binding affinity, the SSB.ssDNA complex is kinetically, but not thermodynamically, stable in the presence of a complementary DNA strand.

In the presence of ATP (i.e. under physiological conditions), RecQ will preferentially start dsDNA unwinding. During dsDNA unwinding catalyzed by RecQ (e.g. during resection of dsDNA ends to initiate homologous recombination) or other processive DNA helicases, free ssDNA is generated to which SSB can bind. Thus, the RecQ-induced SSB binding mode conversion, while enabling efficient initiation of dsDNA unwinding *in vivo*, is unlikely to lead to dissociation of SSB from DNA. In theory binding of SSB to ssDNA can enhance the unwinding activity of these helicases, regardless of the physical interaction between the proteins, due to inhibition of DNA rezipping and helicase backtracking. Here we show that the RecQ–SSB interaction itself has a modest effect on the catalytic activities of RecQ (Figure 6.). The single-molecule helicase unwinding experiments show that even a low concentration of SSB (50 pM) is sufficient to stimulate the unwinding activity of RecQ, through a roughly two-fold decrease in initiation time of unwinding events (Figure 6C). This is consistent with previous ensemble measurements of SSB stimulation of RecQ (7,35,62) and supports the assumption that SSB recruits RecQ to ssDNA–dsDNA junctions. Our single molecule assay also allows us to detect small but significant changes in unwinding rate that would be indistinguishable in ensemble assays (Figure 6D). Whereas the increase in RecQ unwinding activity seen in the presence of SSB is modest, it is present throughout unwinding traces. No such increase is observed for SSBdC (Figure 6C). This suggests that SSB has a secondary role in stimulating RecQ that is dependent on the interaction between the two proteins. The short lifetime of the interaction (Figures 4–6) makes it unlikely that, during unwinding, RecQ would maintain its interaction with a given SSB tetramer. In contrast, a series of new SSB molecules can bind to ssDNA in the wake of the proceeding helicase. This binding could be facilitated by the RecQ–SSB interaction, although ssDNA binding by SSB is rapid in itself. Since the RecQ interaction stabilizes SSB in the 35-nt mode, it is conceivable that during unwinding RecQ serves as a loader of SSB specifically in the 35-nt binding mode to facilitate the formation of a cooperative SSB–ssDNA filament.

In summary, our comprehensive study reveals a model in which (i) ssDNA-bound SSB binds RecQ via its CTP; (ii) This interaction induces a change in the ssDNA-binding mode of SSB that allows RecQ access to the ssDNA–dsDNA junction; (iii) The interaction with RecQ increases its ssDNA affinity and catalytic rate. Together these events afford RecQ access to SSB-coated ssDNA (Figure 7). Whereas our results are pertinent to the SSB–RecQ complex, given the fact that SSB binds and regulates diverse proteins, it is likely that aspects of this reciprocal interaction are universal. Eukaryotic nuclear ssDNA-binding proteins also utilize multiple OB folds to bind ssDNA. Although their structure markedly differs from those of canonical bacterial SSBs, and they lack the C-terminal element that serves as the protein-protein interaction site in bacterial SSBs, eukaryotic ssDNA-binding proteins also interact with numerous proteins with moderate affinity. Human replication protein A (RPA) has multiple known *in vitro* ssDNA binding modes. These similarities with prokaryotic SSB support the possibility of a conserved mechanism in which the RPA binding mode is altered via protein-protein interactions mediated by a structural element functionally similar to the SSB CTP. Indeed, protein-protein interaction-mediated ssDNA binding mode changes have been proposed for human RPA (46,73).

SUPPLEMENTARY DATA

Supplementary Data are available at NAR Online.

ACKNOWLEDGEMENTS

We are grateful to Dr Marie-Paule Strub for assistance with protein expression and purification.
Author contributions: M. Mills, G.M.H., Y.S., M.G., M.K. and K.C.N. conceived and designed the work. M. Mills, G.M.H., Y.S., M.G., M. Martina and K.J.Z. performed experiments. M. Mills, G.M.H., Y.S., M.K. and K.C.N. analyzed data and wrote the paper.

FUNDING

Intramural Research Program of the National Heart, Lung and Blood Institute, National Institutes of Health [HL001056-07 to K.C.N.]; Human Frontier Science Program [RGY0072/2010 to M.K. and K.C.N.]; 'Momentum' Program of the Hungarian Academy of Sciences [LP2011-006/2011 ELTE [KMOP-4.2.1/B-10-2011-0002]; NKFIH [K-116072]; NKFIH [ERC_HU 117680 to M.K.]; Premium Postdoctoral Fellowship Program [PP_460022 to G.M.H.]

of the Hungarian Academy of Sciences. Funding for open access charge: National Institutes of Health [HL001056-07 to K.C.N.].
Conflict of interest statement. None declared.

REFERENCES

1. Kowalczykowski,S.C., Bear,D.G. and Von Hippel,P.H. (1981) Single-stranded DNA binding proteins. *Enzymes*, **14**, 373–444.
2. Chase,J.W. and Williams,K.R. (1986) Single-stranded DNA binding proteins required for DNA replication. *Annu. Rev. Biochem.*, **55**, 103–136.
3. Meyer,R.R. and Laine,P.S. (1990) The single-stranded DNA-binding protein of Escherichia coli. *Microbiol. Rev.*, **54**, 342–380.
4. Chrysogelos,S. and Griffith,J. (1982) Escherichia coli single-strand binding protein organizes single-stranded DNA in nucleosome-like units. *Proc. Natl. Acad. Sci. U.S.A.*, **79**, 5803–5807.
5. Anderson,D.G. and Kowalczykowski,S.C. (1998) SSB protein controls RecBCD enzyme nuclease activity during unwinding: a new role for looped intermediates. *J. Mol. Biol.*, **282**, 275–285.
6. Cadman,C.J. and McGlynn,P. (2004) PriA helicase and SSB interact physically and functionally. *Nucleic Acids Res.*, **32**, 6378–6387.
7. Shereda,R.D., Bernstein,D.A. and Keck,J.L. (2007) A central role for SSB in Escherichia coli RecQ DNA helicase function. *J. Biol. Chem.*, **282**, 19247–19258.
8. Lecointe,F., Sérèna,C., Velten,M., Costes,A., McGovern,S., Meile,J.-C., Errington,J., Ehrlich,S.D., Noirot,P. and Polard,P. (2007) Anticipating chromosomal replication fork arrest: SSB targets repair DNA helicases to active forks. *EMBO J.*, **26**, 4239–4251.
9. Lu,D. and Keck,J.L. (2008) Structural basis of Escherichia coli single-stranded DNA-binding protein stimulation of exonuclease I. *Proc. Natl. Acad. Sci. U.S.A.*, **105**, 9169–9174.
10. Costes,A., Lecointe,F., McGovern,S., Quevillon-Cheruel,S. and Polard,P. (2010) The C-terminal domain of the bacterial SSB protein acts as a DNA maintenance hub at active chromosome replication forks. *PLoS Genet.*, **6**, e1001238.
11. Ryzhikov,M., Koroleva,O., Postnov,D., Tran,A. and Korolev,S. (2011) Mechanism of RecO recruitment to DNA by single-stranded DNA binding protein. *Nucleic Acids Res.*, doi:10.1093/nar/gkr199.
12. Roy,R., Kozlov,A.G., Lohman,T.M. and Ha,T. (2009) SSB protein diffusion on single-stranded DNA stimulates RecA filament formation. *Nature*, **461**, 1092–1097.
13. Bhattacharyya,B., George,N.P., Thurmes,T.M., Zhou,R., Jani,N., Wessel,S.R., Sandler,S.J., Ha,T. and Keck,J.L. (2014) Structural mechanisms of PriA-mediated DNA replication restart. *Proc. Natl. Acad. Sci. U.S.A.*, **111**, 1373–1378.
14. Kozlov,A.G., Jezewska,M.J., Bujalowski,W. and Lohman,T.M. (2010) Binding Specificity of E. coli SSB protein for the χ subunit of DNA pol III Holoenzyme and PriA helicase. *Biochemistry (Mosc.)*, **49**, 3555–3566.
15. Inoue,J., Nagae,T., Mishima,M., Ito,Y., Shibata,T. and Mikawa,T. (2011) A mechanism for single-stranded DNA-binding protein (SSB) displacement from single-stranded DNA upon SSB-RecO interaction. *J. Biol. Chem.*, **286**, 6720–6732.
16. Sun,Z., Tan,H.Y., Bianco,P.R. and Lyubchenko,Y.L. (2015) Remodeling of RecG helicase at the DNA replication fork by SSB protein. *Sci. Rep.*, **5**, 9625.
17. Shereda,R.D., Reiter,N.J., Butcher,S.E. and Keck,J.L. (2009) Identification of the SSB binding site on E. coli RecQ reveals a conserved surface for binding SSB's C terminus. *J. Mol. Biol.*, **386**, 612–625.
18. Raghunathan,S., Ricard,C.S., Lohman,T.M. and Waksman,G. (1997) Crystal structure of the homo-tetrameric DNA binding domain of Escherichia coli single-stranded DNA-binding protein determined by multiwavelength x-ray diffraction on the selenomethionyl protein at 2.9-Å resolution. *Proc. Natl. Acad. Sci. U.S.A.*, **94**, 6652–6657.
19. Raghunathan,S., Kozlov,A.G., Lohman,T.M. and Waksman,G. (2000) Structure of the DNA binding domain of E. coli SSB bound to ssDNA. *Nat. Struct. Mol. Biol.*, **7**, 648–652.
20. Savvides,S.N., Raghunathan,S., Fütterer,K., Kozlov,A.G., Lohman,T.M. and Waksman,G. (2004) The C-terminal domain of full-length E. coli SSB is disordered even when bound to DNA. *Protein Sci. Publ. Protein Soc.*, **13**, 1942–1947.
21. Bujalowski,W. and Lohman,T.M. (1986) Escherichia coli single-strand binding protein forms multiple, distinct complexes with single-stranded DNA. *Biochemistry (Mosc.)*, **25**, 7799–7802.
22. Overman,L.B., Bujalowski,W. and Lohman,T.M. (1988) Equilibrium binding of Escherichia coli single-strand binding protein to single-stranded nucleic acids in the (SSB)65 binding mode. Cation and anion effects and polynucleotide specificity. *Biochemistry (Mosc.)*, **27**, 456–471.
23. Lohman,T.M. and Ferrari,M.E. (1994) Escherichia coli single-stranded DNA-binding protein: multiple DNA-binding modes and cooperativities. *Annu. Rev. Biochem.*, **63**, 527–570.
24. Ferrari,M.E., Bujalowski,W. and Lohman,T.M. (1994) Co-operative Binding of Escherichia coli SSB Tetramers to Single-stranded DNA in the (SSB)35 Binding Mode. *J. Mol. Biol.*, **236**, 106–123.
25. Roy,R., Kozlov,A.G., Lohman,T.M. and Ha,T. (2007) Dynamic structural rearrangements between DNA binding modes of E. coli SSB protein. *J. Mol. Biol.*, **369**, 1244–1257.
26. Suksombat,S., Khafizov,R., Kozlov,A.G., Lohman,T.M. and Chemla,Y.R. (2015) Structural dynamics of E. coli single-stranded DNA binding protein reveal DNA wrapping and unwrapping pathways. *eLife*, **4**, e08193.
27. Antony,E., Weiland,E., Yuan,Q., Manhart,C.M., Nguyen,B., Kozlov,A.G., McHenry,C.S. and Lohman,T.M. (2013) Multiple C-terminal tails within a single E. coli SSB homotetramer coordinate DNA replication and repair. *J. Mol. Biol.*, **425**, 4802–4819.
28. Huang,Y.-H., Huang,C.-Y., Huang,Y.-H. and Huang,C.-Y. (2014) C-terminal domain swapping of SSB changes the size of the ssDNA binding site, C-terminal domain swapping of SSB changes the size of the ssDNA binding site. *BioMed Res. Int. BioMed Res. Int.*, **2014**, e573936.
29. Curth,U., Genschel,J., Urbanke,C. and Greipel,J. (1996) In vitro and in vivo function of the C-terminus of Escherichia coli single-stranded DNA binding protein. *Nucleic Acids Res.*, **24**, 2706–2711.
30. Hickson,I.D. (2003) RecQ helicases: caretakers of the genome. *Nat. Rev. Cancer*, **3**, 169–178.
31. Bernstein,K.A., Gangloff,S. and Rothstein,R. (2010) The RecQ DNA helicases in DNA repair. *Annu. Rev. Genet.*, **44**, 393–417.
32. Croteau,D.L., Popuri,V., Opresko,P.L. and Bohr,V.A. (2014) Human RecQ helicases in DNA repair, recombination, and replication. *Annu. Rev. Biochem.*, **83**, 519–552.
33. Dou,S.-X., Wang,P.-Y., Xu,H.Q. and Xi,X.G. (2004) The DNA binding properties of the Escherichia coli RecQ helicase. *J. Biol. Chem.*, **279**, 6354–6363.
34. Harmon,F.G., DiGate,R.J. and Kowalczykowski,S.C. (1999) RecQ helicase and topoisomerase III comprise a novel DNA strand passage function: a conserved mechanism for control of DNA recombination. *Mol. Cell*, **3**, 611–620.
35. Harmon,F.G. and Kowalczykowski,S.C. (2001) Biochemical characterization of the DNA helicase activity of the Escherichia coli RecQ helicase. *J. Biol. Chem.*, **276**, 232–243.
36. Harmon,F.G., Brockman,J.P. and Kowalczykowski,S.C. (2003) RecQ helicase stimulates both DNA catenation and changes in DNA topology by topoisomerase III. *J. Biol. Chem.*, **278**, 42668–42678.
37. Suski,C. and Marians,K.J. (2008) Resolution of converging replication forks by RecQ and topoisomerase III. *Mol. Cell*, **30**, 779–789.
38. Rong,S.B., Väliaho,J. and Vihinen,M. (2000) Structural basis of Bloom syndrome (BS) causing mutations in the BLM helicase domain. *Mol. Med. Camb. Mass*, **6**, 155–164.
39. Mohaghegh,P., Karow,J.K., Brosh,R.M. Jr, Bohr,V.A. and Hickson,I.D. (2001) The Bloom's and Werner's syndrome proteins are DNA structure-specific helicases. *Nucleic Acids Res.*, **29**, 2843–2849.
40. Bernstein,D.A., Zittel,M.C. and Keck,J.L. (2003) High-resolution structure of the E.coli RecQ helicase catalytic core. *EMBO J.*, **22**, 4910–4921.
41. Harami,G.M., Gyimesi,M. and Kovács,M. (2013) From keys to bulldozers: expanding roles for winged helix domains in nucleic-acid-binding proteins. *Trends Biochem. Sci.*, **38**, 364–371.
42. Harami,G.M., Nagy,N.T., Martina,M., Neuman,K.C. and Kovács,M. (2015) The HRDC domain of E. coli RecQ helicase controls single-stranded DNA translocation and double-stranded DNA unwinding rates without affecting mechanoenzymatic coupling. *Sci. Rep.*, **5**, 11091.

43. Harami,G.M., Seol,Y., In,J., Ferencziová,V., Martina,M., Gyimesi,M., Sarlós,K., Kovács,Z.J., Nagy,N.T., Sun,Y. *et al.* (2017) Shuttling along DNA and directed processing of D-loops by RecQ helicase support quality control of homologous recombination. *Proc. Natl. Acad. Sci. U.S.A.*, doi:10.1073/pnas.1615439114.
44. Killoran,M.P. and Keck,J.L. (2006) Sit down, relax and unwind: structural insights into RecQ helicase mechanisms. *Nucleic Acids Res.*, **34**, 4098–4105.
45. Vindigni,A., Marino,F. and Gileadi,O. (2010) Probing the structural basis of RecQ helicase function. *Biophys. Chem.*, **149**, 67–77.
46. Fanning,E., Klimovich,V. and Nager,A.R. (2006) A dynamic model for replication protein A (RPA) function in DNA processing pathways. *Nucleic Acids Res.*, **34**, 4126–4137.
47. Chen,H., Lisby,M. and Symington,L.S. (2013) RPA coordinates DNA end resection and prevents formation of DNA hairpins. *Mol. Cell*, **50**, 589–600.
48. Doherty,K.M., Sommers,J.A., Gray,M.D., Lee,J.W., von Kobbe,C., Thoma,N.H., Kureekattil,R.P., Kenny,M.K. and Brosh,R.M. (2005) Physical and functional mapping of the replication protein A interaction domain of the Werner and Bloom Syndrome helicases. *J. Biol. Chem.*, **280**, 29494–29505.
49. Opresko,P.L., Laine,J.-P., Brosh,R.M., Seidman,M.M. and Bohr,V.A. (2001) Coordinate action of the helicase and 3′ to 5′ exonuclease of Werner Syndrome protein. *J. Biol. Chem.*, **276**, 44677–44687.
50. Sarlós,K., Gyimesi,M. and Kovács,M. (2012) RecQ helicase translocates along single-stranded DNA with a moderate processivity and tight mechanochemical coupling. *Proc. Natl. Acad. Sci. U.S.A.*, **109**, 9804–9809.
51. Kocsis,Z.S., Sarlós,K., Harami,G.M., Martina,M. and Kovács,M. (2014) A nucleotide-dependent and HRDC domain-dependent structural transition in DNA-bound RecQ helicase. *J. Biol. Chem.*, **289**, 5938–5949.
52. Seol,Y., Strub,M.-P. and Neuman,K.C. (2016) Single molecule measurements of DNA helicase activity with magnetic tweezers and t-test based step-finding analysis. *Methods San Diego Calif*, **105**, 119–127.
53. Lohman,T.M., Green,J.M. and Beyer,R.S. (1986) Large-scale overproduction and rapid purification of the Escherichia coli ssb gene product. Expression of the ssb gene under lambda PL control. *Biochemistry (Mosc.)*, **25**, 21–25.
54. Dillingham,M.S., Tibbles,K.L., Hunter,J.L., Bell,J.C., Kowalczykowski,S.C. and Webb,M.R. (2008) Fluorescent single-stranded DNA binding protein as a probe for sensitive, real-time assays of helicase activity. *Biophys. J.*, **95**, 3330–3339.
55. Gyimesi,M., Harami,G.M., Sarlós,K., Hazai,E., Bikádi,Z. and Kovács,M. (2012) Complex activities of the human Bloom's syndrome helicase are encoded in a core region comprising the RecA and Zn-binding domains. *Nucleic Acids Res.*, **40**, 3952–3963.
56. Johnson,K.A., Simpson,Z.B. and Blom,T. (2009) Global Kinetic Explorer: a new computer program for dynamic simulation and fitting of kinetic data. *Anal. Biochem.*, **387**, 20–29.
57. Kozlov,A.G., Cox,M.M. and Lohman,T.M. (2010) Regulation of single-stranded DNA binding by the C termini of Escherichia coli single-stranded DNA-binding (SSB) protein. *J. Biol. Chem.*, **285**, 17246–17252.
58. Kunzelmann,S., Morris,C., Chavda,A.P., Eccleston,J.F. and Webb,M.R. (2010) Mechanism of interaction between single-stranded DNA binding protein and DNA. *Biochemistry (Mosc.)*, **49**, 843–852.
59. Rad,B. and Kowalczykowski,S.C. (2012) Efficient coupling of ATP hydrolysis to translocation by RecQ helicase. *Proc. Natl. Acad. Sci. U.S.A.*, **109**, 1443–1448.
60. Zhang,X.-D., Dou,S.-X., Xie,P., Hu,J.-S., Wang,P.-Y. and Xi,X.G. (2006) Escherichia coli RecQ is a rapid, efficient, and monomeric helicase. *J. Biol. Chem.*, **281**, 12655–12663.
61. Xu,H.Q., Deprez,E., Zhang,A.H., Tauc,P., Ladjimi,M.M., Brochon,J.-C., Auclair,C. and Xi,X.G. (2003) The Escherichia coli RecQ helicase functions as a monomer. *J. Biol. Chem.*, **278**, 34925–34933.
62. Umezu,K. and Nakayama,H. (1993) RecQ DNA helicase of Escherichia coli. *J. Mol. Biol.*, **230**, 1145–1150.
63. Seol,Y. and Neuman,K. (2011) Magnetic tweezers for single-molecule manipulation. In: Peterman,EJG and Wuite,GJL (eds). *Single Molecule Analysis, Methods in Molecular Biology*. Humana Press, pp. 265–293.
64. Hishida,T., Han,Y.-W., Shibata,T., Kubota,Y., Ishino,Y., Iwasaki,H. and Shinagawa,H. (2004) Role of the Escherichia coli RecQ DNA helicase in SOS signaling and genome stabilization at stalled replication forks. *Genes Dev.*, **18**, 1886–1897.
65. Morimatsu,K. and Kowalczykowski,S.C. (2014) RecQ helicase and RecJ nuclease provide complementary functions to resect DNA for homologous recombination. *Proc. Natl. Acad. Sci. U.S.A.*, **111**, E5133–E5142.
66. Harmon,F.G. and Kowalczykowski,S.C. (1998) RecQ helicase, in concert with RecA and SSB proteins, initiates and disrupts DNA recombination. *Genes Dev.*, **12**, 1134–1144.
67. Waldman,V.M., Weiland,E., Kozlov,A.G. and Lohman,T.M. (2016) Is a fully wrapped SSB–DNA complex essential for Escherichia coli survival? *Nucleic Acids Res.*, **44**, 4317–4329.
68. Wessel,S.R., Marceau,A.H., Massoni,S.C., Zhou,R., Ha,T., Sandler,S.J. and Keck,J.L. (2013) PriC-mediated DNA replication restart requires PriC complex formation with the single-stranded DNA-binding protein. *J. Biol. Chem.*, **288**, 17569–17578.
69. Shereda,R.D., Kozlov,A.G., Lohman,T.M., Cox,M.M. and Keck,J.L. (2008) SSB as an organizer/mobilizer of genome maintenance complexes. *Crit. Rev. Biochem. Mol. Biol.*, **43**, 289–318.
70. Kozlov,A.G., Weiland,E., Mittal,A., Waldman,V., Antony,E., Fazio,N., Pappu,R.V. and Lohman,T.M. (2015) Intrinsically disordered C-terminal tails of E. coli single-stranded DNA binding protein regulate cooperative binding to single-stranded DNA. *J. Mol. Biol.*, **427**, 763–774.
71. Zhou,R., Kozlov,A.G., Roy,R., Zhang,J., Korolev,S., Lohman,T.M. and Ha,T. (2011) SSB functions as a sliding platform that migrates on DNA via reptation. *Cell*, **146**, 222–232.
72. Kozlov,A.G. and Lohman,T.M. (2002) Stopped-flow studies of the kinetics of single-stranded DNA binding and wrapping around the Escherichia coli SSB tetramer. *Biochemistry (Mosc.)*, **41**, 6032–6044.
73. Fan,J. and Pavletich,N.P. (2012) Structure and conformational change of a replication protein A heterotrimer bound to ssDNA. *Genes Dev.*, **26**, 2337–2347.